Investigation of the Three-Dimensional Turbulent Flow Fields of the Gas Swirl Burner with a Cone Type Baffle Plate (Ⅱ)

Jang-kweon Kim*

Department of Marine Engineering, Kunsan National University, Chonbuk 573-702, Korea

This paper presents three-dimensional mean velocities, turbulent intensities and Reynolds shear stresses measured in the Y-Z plane of the gas swirl burner with a cone type baffle plate by using an X-type hot-wire probe. This experiment is carried out at the flow rate of 450 ℓ/min which is equivalent to the combustion air flow rate necessary to heat release 15,000 kcal/hr in a gas furnace. Mean velocities and turbulent intensities etc. show that their maximum values exist around the narrow slits situated radially on the edge of and in front of a burner. According to downstream regions, they have a peculiar shape like a starfish because the flows going out of the narrow slits and the swirl vanes of an inclined baffle plate diffuse and develop into inward and outward of a burner. The rotational flow due to the inclined flow velocity going out of swirl vanes of a cone type baffle plate seems to decrease the magnitudes of mean velocities V and W respectively by about 30 % smaller than those of mean velocity U. The turbulent intensities have large values of 50 %~210 % within the range of $0.5<r/R<1$ and around the narrow slits in front of a burner because the large transverse slope of axial mean velocity remains in these region. Therefore, the combustion reaction is expected to occur actively near these regions. Moreover, the Reynolds shear stresses are largely distributed near the narrow slits of a burner.

Key Words : Gas Swirl Burner, Hot-Wire Anemometer, Subsonic Wind Tunnel, Turbulent Flow Fields, X-Probe

Nomenclature

KE	: Turbulent kinetic energy $\{KE=\frac{1}{2}(u^2+v^2+w^2)\}$ [m²/s²]
Q	: Air flow rate [m³/min]
R	: Radius of a swirl burner [m]
U, V, W	: Mean velocity component in the X, Y and Z direction respectively [m/s]
u, v, w	: Root mean square of turbulent fluctuation velocity in the X, Y and Z direction respectively [m/s]
u^2, v^2, w^2	: Reynolds normal stresses or variances of turbulence in the X, Y and Z direction respectively [m²/s²]
U_o	: Upstream mean velocity of a swirl burner ($=Q/\pi R^2$) [m/s]
uv, uw	: Reynolds shear stress components [m²/s²]
X, Y, Z	: Distance and direction of cartesian coordinate system

* **E-mail** : flowkim@kunsan.ac.kr
TEL : +82-63-469-1848 ; **FAX** : +82-63-469-1841
Department of Marine Engineering, Kunsan National University, 1044-2, So-ryong Dong, Kunsan, Chonbuk 573-702, Korea. (Manuscript **Received** September 2, 2000; **Revised** March 8, 2001)

1. Introduction

Generally, fluid dynamics plays an important role in mixing and transport properties in flames as well as in the supply and exhaust duct of combustors. The most effective means for controlling flame shape and length is to change the aerodynamic flow patterns through burners. Typically, fuel and oxidant are initially separated before burning, but subsequently they mixed by turbulent jet flows, swirlers and generation of

recirculation zones. The interaction between turbulence and chemical kinetics is one of the most challenging problems in combustion science. Turbulence enhances rates of chemical reaction by increasing transport properties for heat, mass and momentum transfer. Here, profiles of velocity, temperature, concentration and fluctuating components are closely interrelated. Especially, high-intensity turbulence increases mixing rates, flame propagation rates and combustion rates of fuel. (Chigier, 1981)

The combustors with swirling flow are widely adopted for a gas turbine, a boiler and an industrial furnace etc. for improving the performance of flame stabilization, short flames and high combustion intensity. For the aerodynamics of swirling flow, it is well clarified in a reference (Beer et al., 1972) that the swirl number representing swirl intensity relates to flow characteristics. On the other hand, for the combustion about swirling flow, it is well classified in some references (Beer et al., 1972; Kihm et al., 1990) that the swirling flow affects the stabilization of flame, combustion intensity and NO_x formation.

Especially, the combustion characteristics of combustors using a gas swirl burner depend on various parameters such as the composition of fuel gas, the diffusion of the ejected gas, and the mixing between air and fuel gas etc. Above all, the mixing rate between air and fuel gas is thought to become more important parameter than the others in combustion state. Moreover, there are many parameters of the angle, the inner and outer radius of a swirl vane and the shape of flame holder as to the optimum parameter for burner design. On the other hand, the efforts for improving combustion property according to change of the geometric shape of a burner are actively progressing at home and abroad through the experimental and theoretical study. The study on the gas burner based on the investigation of flow fields and atomization of a gun type oil burner using kerosene as a liquid fuel is well done abroad, while there are very few materials available on both a gas burner and a gun type oil burner at home.

Aoki et al. (1988, 1989) experimentally clarified the location, size and shape of recirculation, the eye of vortex and sub-recirculation zones for the swirling numbers, and the maximum reverse flow rate of recirculation zone on the circular duct flow superposed with swirling flow. In order to analyze these results, they used flow visualization by spark tracing method for clearing flow patterns, five-hole pitot-tube, and LDA (Laser Doppler Anemometer) system for measuring three time-mean velocities and turbulent characteristics respectively when the swirling numbers change from zero to 1.35 by an axial flow type swirler.

Ikeda et al. (1995) measured a flow velocity and gas species in combustion and non-combustion in an oil furnace by using LDA system. They showed that the reversing flow regions for both cases were located at the same place and their volumes were almost equal.

Kihm et al. (1990) investigated the flow characteristics of turbulent swirling flows according to change of a hub diameter and a vane angle of swirler for a gas turbine by using LDA system. They observed that the peak tangential velocities were found at the exit of the swirler of a vane angle 40°. These findings agreed to the result of direct force measurements of thrust and torque. In other words, they were found to be higher for the swirler of 40° than for the swirlers of 20° and 60°. The size and the strength of a recirculation zone were found to be highest at the swirler of 40°.

Kim et al. (1997, 1998) and Yoon (1999) introduced the experimental and numerical method to compare characteristics of flow fields with those of combustion fields according to the shape of flame holder with a vertical and an inclined baffle plate in a gun type oil and gas burner. They also verified that the flame holder with an inclined baffle plate formed more stable flame structure than that with a vertical baffle plate in the inner downstream region, and what is more, the hot temperature region attained in the downstream region of the swirl vane and the narrow slits situated radially on the edge of a burner respectively.

Although we only investigate the flow fields measured in the X-Y plane of a gas swirl burner

in Part I of this paper (Kim, 2001), we cannot understand at all the complete flow characteristics formed in the Y-Z plane of this burner. Therefore, in the present study, the mean velocity, the turbulent intensity, the turbulent kinetic energy and the Reynolds shear stress were measured and analyzed in the Y-Z plane of three-dimensional turbulent flow fields formed from the gas swirl burner with a cone type baffle plate without flame and combustion chamber by using an X type hot-wire probe. These measurements were only achieved at the combustion air flow rate of 450 ℓ/min because the non-dimensional characteristics between the results according to the variation of velocity generally had a similar shape. (Kim et al., 2001)

The objective of this study is to grasp both the flow characteristics and the questions on the gas swirl burner with a cone type baffle plate. Afterwards, these design materials are due to use for the development of a new model after maintaining the optimum design data obtained from a conventional model. (Kim, 2001)

2. Experimental Apparatus

Figure 1 indicates the detail structure of the gas swirl burner with a cone type baffle plate used in this study. This burner is due to apply in a gas furnace for home-appliance unit with heat release 15,000 kcal/hr.

This gas swirl burner is the same thing as it used in Part I of this paper, and it is characterized by the shape of a burner with the cone type baffle plate which is inclined about 45° to the front side of a circular tube. This cone type baffle plate is composed of eight swirl vanes located in the inclined baffle plate and eight narrow slits situated radially on the edge of the swirl burner that is just located above a swirl vane. This swirl burner has an geometric swirl number (Beer et al., 1972) of 0.34. (Kim, 2001)

Here, it can be thought that this gas swirl burner guides both circulation flow and swirl flow at the same time by eight swirl vanes located in the inclined plane and eight narrow slits situ-

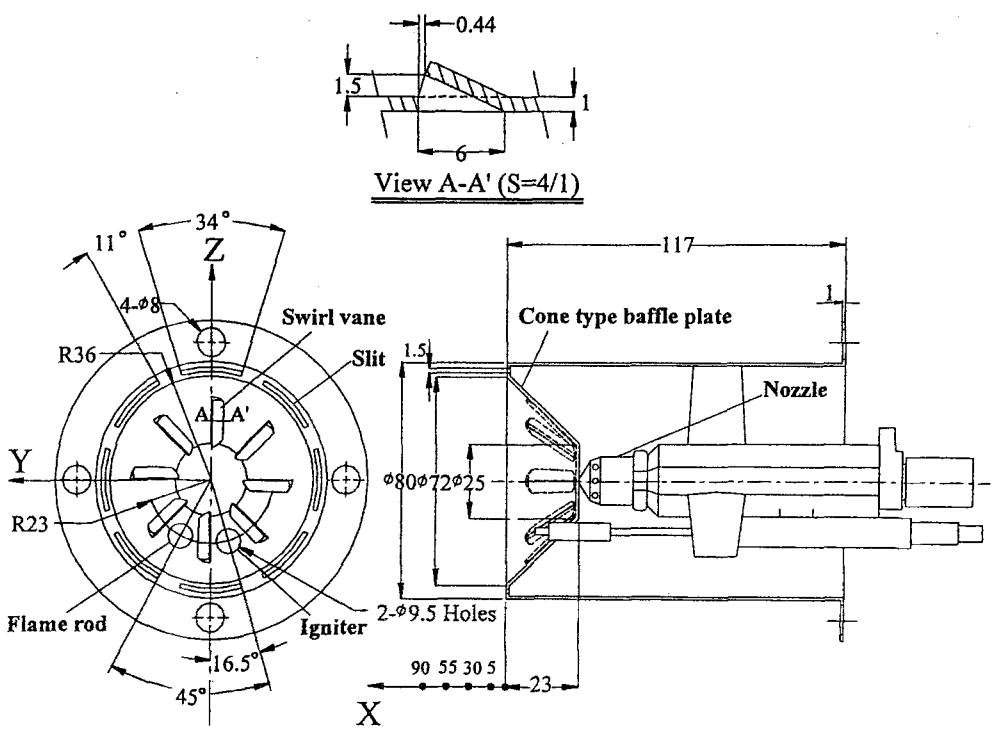

Fig. 1 Configuration of a gas swirl burner

ated radially on the edge of a swirl burner. However, because this burner has a comparatively small swirl number and the mean velocity at the narrow slits has a value larger than that at swirl vanes, this burner can be considered to adopt the shape that generates the intense mixing between fuel gas and oxygen through strong turbulent intensity formed by a large transverse slope of axial mean velocity at narrow slits rather than at swirl vanes.

In order to carry out the measurements, we used a subsonic wind tunnel having a performance of turbulent intensity under about 0.02 % at mean flow velocity 15 m/s, a three-dimensional hot-wire anemometer system (Dantec 90N10 Streamline) which is composed of three constant temperature hot-wire anemometers, a calibrator (Dantec 90H01 & 90H02), three-dimensional automatic traversing system (Dantec 41T50 & 41T75) and a personal computer. (Kim, 2001)

3. Experimental Method

The measurement of three-dimensional velocity (Bruun, 1996; Dantec, 2000) accomplished in this study by using X-probe (Dantec, 55R51) from the hot-wire anemometer system and the personal computer is carried out through the same method as it used in Part Ⅰ of this paper. (Kim, 2001) The exit velocities of the swirl burner used in this study were controlled under the static pressure of 164 Pa collected from four pressure taps attached on the surface of circular tube of a swirl burner connected with the test section of a subsonic wind tunnel. Here, this static pressure corresponds to the flow rate of 450 ℓ/min which is utilized for actual combustion air flow rate. The normal velocity measurements were carried out by sampling enough many data from turbulent flow fields formed at the respective measuring position in the Y-Z plane after the oscillation of velocity obtained from subsonic wind tunnel mostly disappears. The sampling frequency and the number of sampling of A/D converter used in this study are controlled with 10 kHz and 102, 400 per channel respectively. Moreover, the frequency of low-pass filter of a signal conditioner was set up with 30 kHz per channel.

The gas swirl burner adopted in this study was used after eliminating flame rod and igniter installed in a cone type baffle plate as shown in Fig. 1 and blocking their holes with a glue vinyl tape. The velocity measurements with respect to X-direction were selected as the four positions of 5, 30, 55 and 90 mm in front of a swirl burner. On the other hand, in order to move X-probe around the Y-Z plane at the respective X-position, the polar coordinate system is adopted to make the grid file for three-dimensional automatic traversing system. Consequently, the measuring position with respect to R-direction was selected from the origin of Y-Z plane to 70 mm at 5 mm intervals per position. Moreover, the measuring position with respect to θ-direction was selected from 0° to 355° at 5-degree intervals per position. Here, because the magnitude of velocity ejected from the eight narrow slits situated radially on the edge of a burner is the largest, the velocity measurement around these narrow slits was carried out with traversing X-probe by 1 mm in order to measure a detailed flow velocity. The room temperature was controlled within about 19±0.5 ℃ for reducing the error of velocity due to the change of temperature at the smallest possible value. In addition, the AVR was used for eliminating the oscillation of velocity in the test section of a subsonic wind tunnel due to the change of voltage.

4. Results and Discussion

4.1 Mean velocity distribution

Figure 2 indicates the non-dimensional mean velocity represented by dividing axial mean velocity U measured in the Y-Z plane at the location of X/R=0.1282, 0.7692, 1.4103 and 2.3077 respectively by upstream mean velocity U_0 of a swirl burner. The mean velocity U shown in Fig. 2(a) is obtained at the initial region of a burner, and it appears to be a symmetric distribution with respect to the origin. Moreover, the mean velocity U shows the magnitude of accelerated velocity having about nine times as large as upstream

mean velocity U_0 because it forms maximum values around $r/R=\pm 0.97$ corresponding to eight narrow slits. Here, the shape of eight narrow slits can also be seen in Fig. 2(a). Moreover, the mean velocity U is distributed with a comparatively large magnitude of above about three times larger than upstream mean velocity U_0 of a burner within the range of $0.5<r/R<1$, and it goes down as the radial distance changes from the outer region to the origin of a burner because the rapid flow ejected from the eight narrow slits and the flow going out of swirl vanes located on the surface of a cone type baffle plate diffuse and develop mutually in the neighborhood. Especially, the streamwise mean velocity U measured in the central region of $0<r/R<0.5$ shows the smallest scale because the inner region of a burner except both inclined swirl vanes and narrow slits has no holes. On the other hand, the maximum values shown in both Fig. 2(b) and Fig. 2(c) are obviously reduced to about quintuple and three times as large as upstream mean velocity U_0 respectively, and Fig. 2(b) especially shows that the mean velocity U is expanded around the respective narrow slit in itself. Moreover, as the measuring X-position increases toward downstream region, the distribution of maximum mean velocity U shows an elongated shape toward the rotating flow direction as a result of the flow diffusion and development facing to the central part as shown in Fig. 2(c). Here, the rotating flow shape of a burner can be also seen in Fig. 2

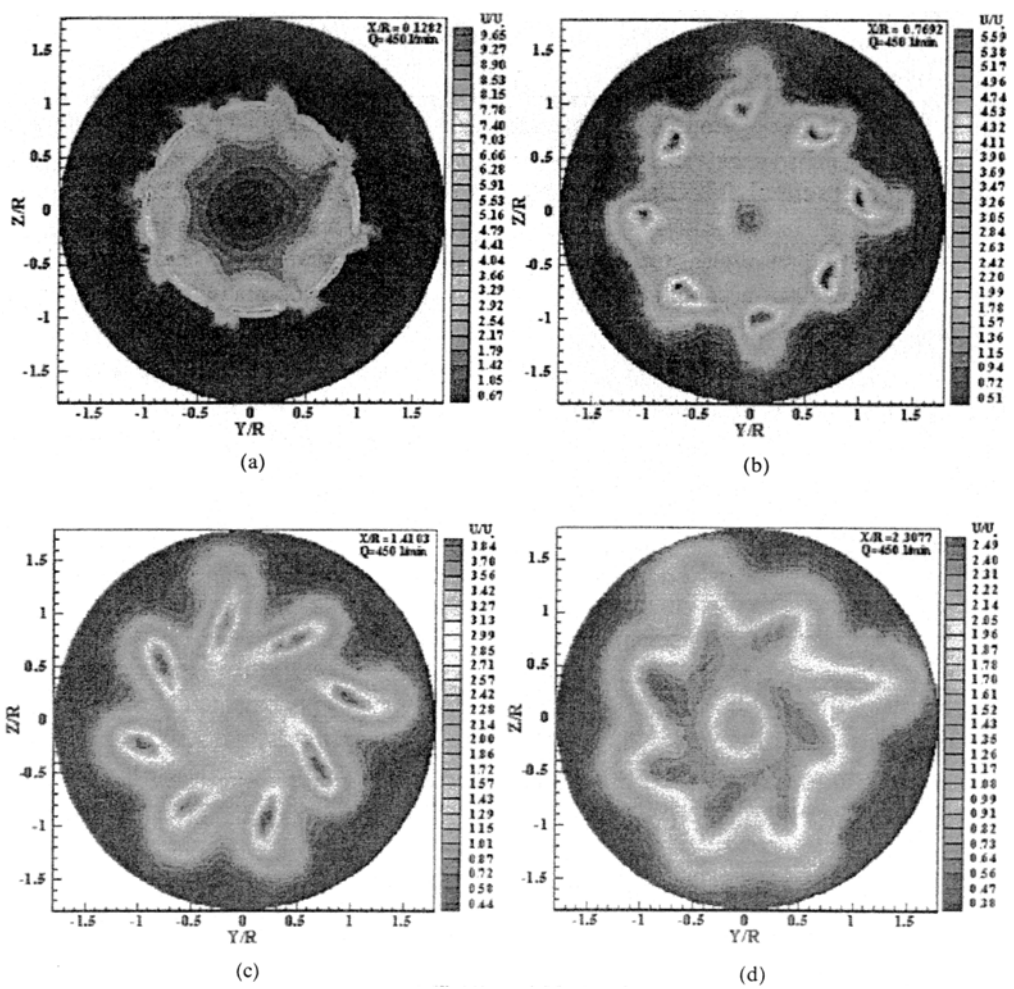

Fig. 2 Mean velocity U profiles in the Y-Z plane

(c) by means of swirl vanes. On the other hand, Fig. 2(d) shows that the mixing phenomena are actively achieved in the range between narrow slits and swirl vanes because the flow develops comparatively fully according to increase of an axial distance. Therefore, the mean velocity U shown in Fig. 2(d) indicates a magnitude of about two times as large as upstream mean velocity U_0 and has the distribution of the shape like a starfish.

Figure 3 indicates the non-dimensional mean velocity represented by dividing Y-directional mean velocity V measured in the Y-Z plane at the location of X/R=0.1282, 0.7692, 1.4103 and 2.3077 respectively by upstream mean velocity U_0 of a swirl burner. The mean velocity V shown in Fig. 3(a) is distributed with a different velocity sign of about quadruple as large as upstream mean velocity near the eight narrow slits. Particularly, the mean velocity V shows a positive maximum velocity distribution in the left part at Y/R=−0.97 of Fig. 3(a) because the flow heads from the right side to the centerline by means of the inclined flow angle of left-hand swirl vane, and vice versa in the right part of at Y/R=0.97 because the flow heads from the left side to the centerline due to the inclined flow angle of the right-hand swirl vane. Here, the mean velocity V in the lower part of Z-axis shown in Fig. 3(a) indicates negative values in the inside region of a burner, and vice versa in the outside region because it rotates clockwise. However, the mean

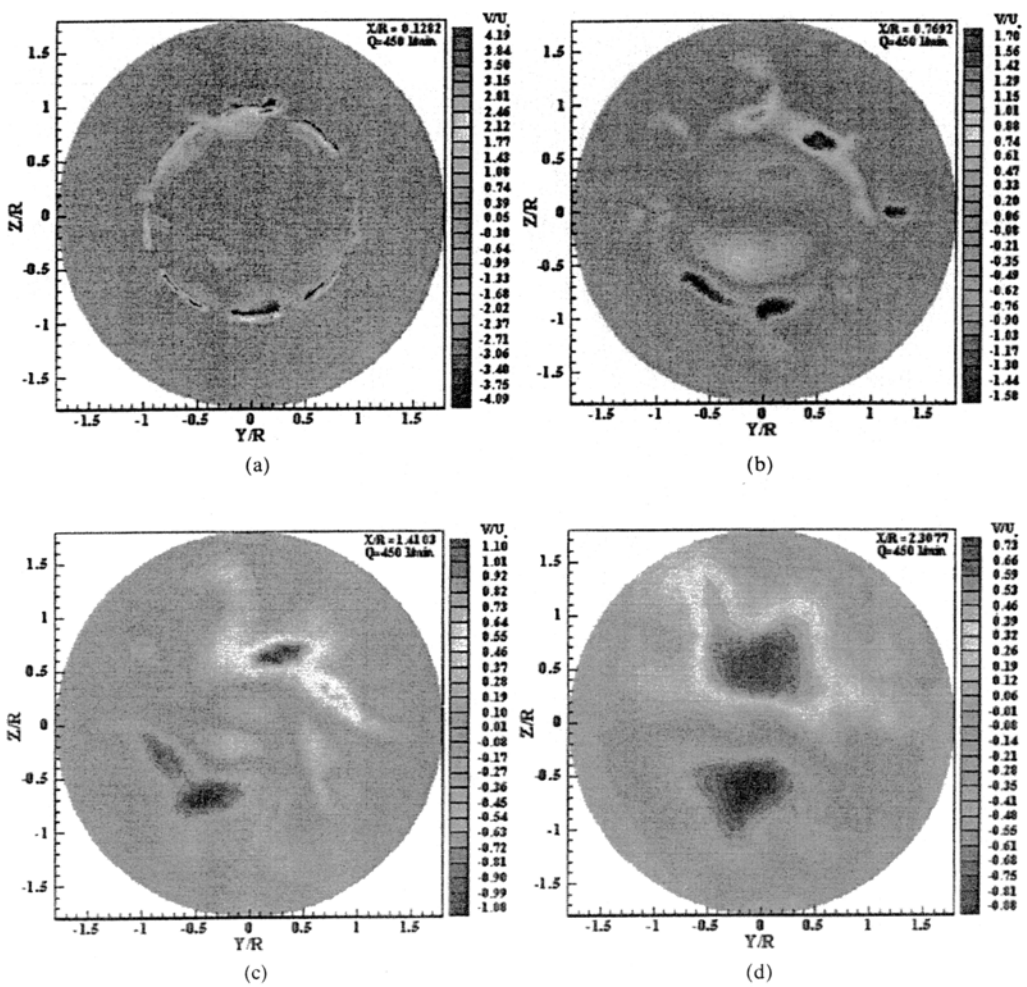

Fig. 3 Mean velocity V profiles in the Y-Z plane

velocity V in the upper part of Z-axis shows positive values in the inside region of a burner, and vice versa in the outside region. As the axial distance increases, the magnitude of mean velocity V is largely reduced as shown in Fig. 3(b), Fig. 3(c), and Fig. 3(d), but it diffuses by means of the mutual mixing phenomena between the flow going out of a swirl vane and the jet flow ejected from the narrow slits. Therefore, the positive peak value of velocity is formed in the upper side of a burner, and vice versa in the lower side. Moreover, the positive and negative velocities are separately distributed in these regions with expanding each velocity into a large region.

Figure 4 shows the non-dimensional mean velocity represented by dividing Z-directional mean velocity W measured in the Y-Z plane at the location of X/R=0.1282, 0.7692, 1.4103 and 2.3077 respectively by upstream mean velocity U_0 of a swirl burner. The mean velocity W measured in the front of a burner as shown in Fig. 4(a) is also distributed with a different velocity sign of about quadruple as large as upstream mean velocity near eight narrow slits, and it has the same velocity as V. Particularly, the mean velocity W indicates a negative maximum velocity distribution at Z/R=0.97 located in the upper side of a burner shown in Fig. 4(a), and vice versa at Z/R=−0.97 located in the lower side. Here, the mean velocity W situated in the flow field of the left side of Y-axis with respect to Z=0 appears as a positive value in the inner side of a burner, and

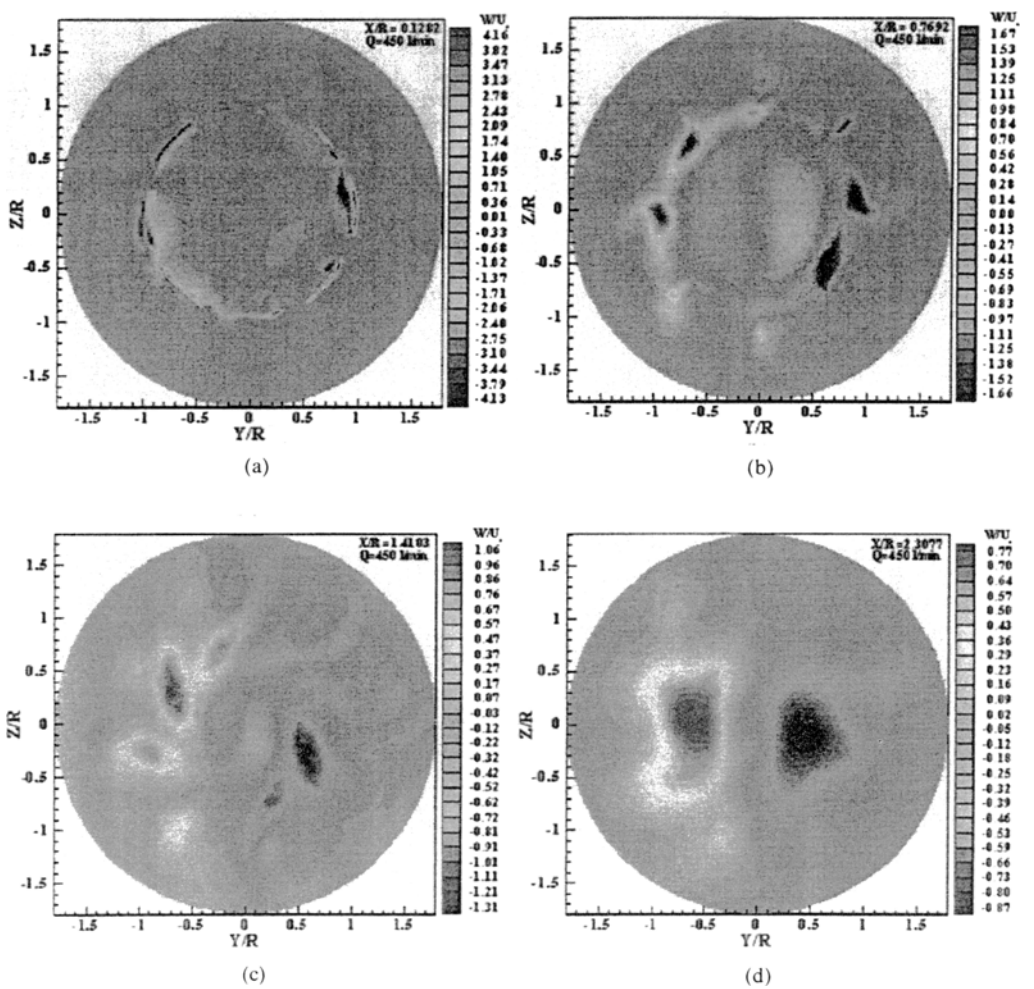

Fig. 4 Mean velocity W profiles in the Y-Z plane

vice versa in the outer side as a result of clockwise rotation of flow. However, the mean velocity W situated in the right side of Y-axis with respect to Z=0 appears as a negative value in the inner side of a burner, and vice versa in the outer side. On the other hand, as the axial distance increases, the mean velocity W as shown in Fig. 4(b), Fig. 4 (c), and Fig. 4(d) is distributed with positive peak velocities in the left side of Y-axis around the narrow slits, and vice versa in the right side as a result of the diffusion due to the mutual mixing between the flow going out of a burner and the flow formed from the narrow slits. Finally, the positive peak velocities as shown in Fig. 4(d) are largely formed in the left side of a burner, and vice versa in the right side.

4.2 Turbulent intensity distribution

Figure 5 shows the non-dimensional turbulent intensity distribution represented by dividing RMS (Root-mean-square) u measured in the Y-Z plane at the location of X/R=0.1282, 0.7692, 1.4103 and 2.3077 respectively by upstream mean velocity U_0 of a swirl burner. The distribution of turbulent intensity u from Fig. 5(a) shows a comparatively symmetric shape with respect to the origin of a burner. Moreover, the turbulent intensity u develops to a large magnitude of above about 160 % around r/R=0.97 corresponding to eight narrow slits. Especially, the turbulent intensity u is largely distributed with a magnitude of above about 71 % within the range of 0.5<r/R<

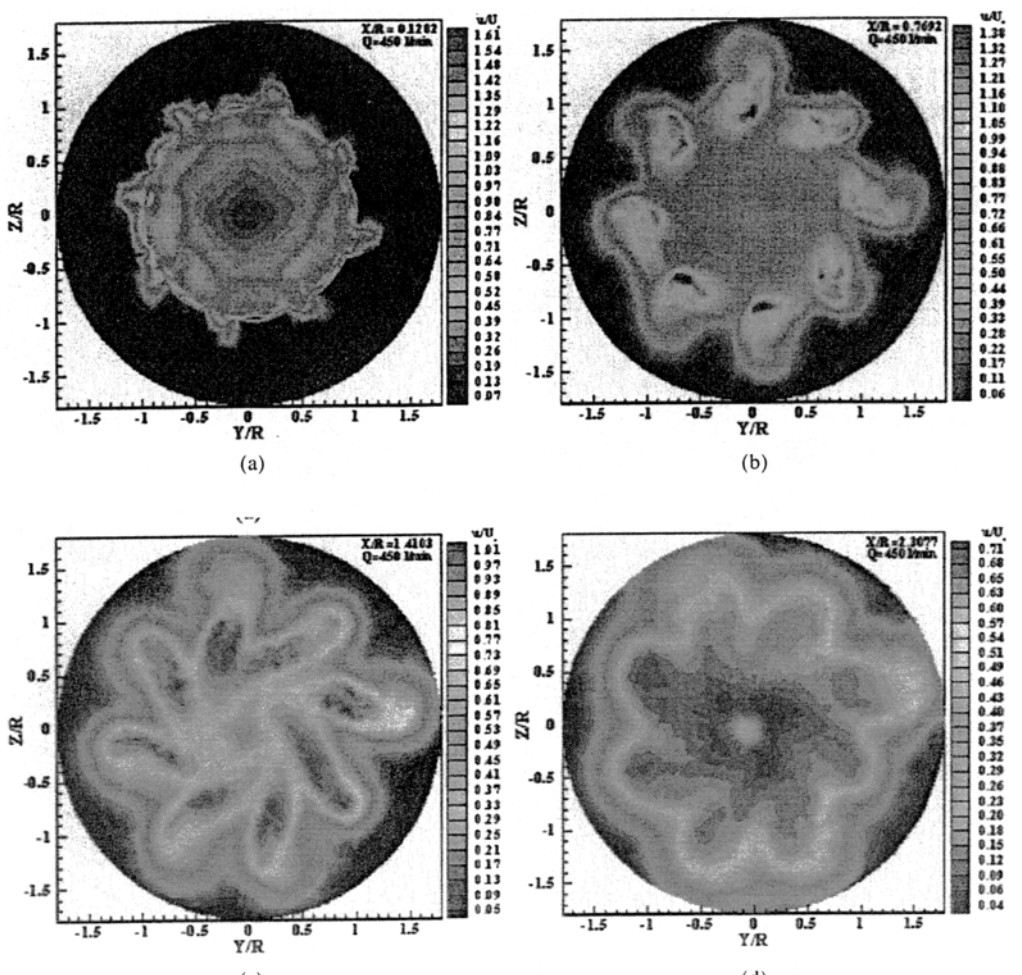

Fig. 5 Turbulent intensity u profiles in the Y-Z plane

1. This reason why the turbulent intensity u indicates comparatively high values in these regions is because the axial mean flow velocity going out of narrow slits is largely distributed, and the transverse slope of axial mean velocity with respect to Y and Z-direction is the largest scale, and what is more, the flow rotation by means of swirl vanes strongly acts in this region. Kihm et al. (1990) early described that the swirler brought about high turbulence intensities having a scale of above 100 %. Besides, the turbulent intensity u in the central region of a burner is smaller than that of the outer side of a burner, and it shows a minimum value of about 10 % near the origin. As shown in Fig. 5(b), the peak value of turbulent intensity u formed around the narrow slits indicates that its range is expanded even though its magnitude is reduced. Moreover, as the axial distance increases, the turbulent intensity u presents an elongated shape toward the rotating flow direction as shown in Fig. 5(c) because the streamwise mean velocity is evidently reduced and the rotational flow due to the swirl vanes is strongly highlighted in this region. Consequently, both the streamwise mean velocity and the rotational flow affect the internal region of a burner. Moreover, the turbulent intensity u represented in Fig. 5(d) is widely distributed with the large magnitude of above about 55 % in the central region of a burner, and it shows a starfish shape due to the effect of narrow slits in the outer region of the burner.

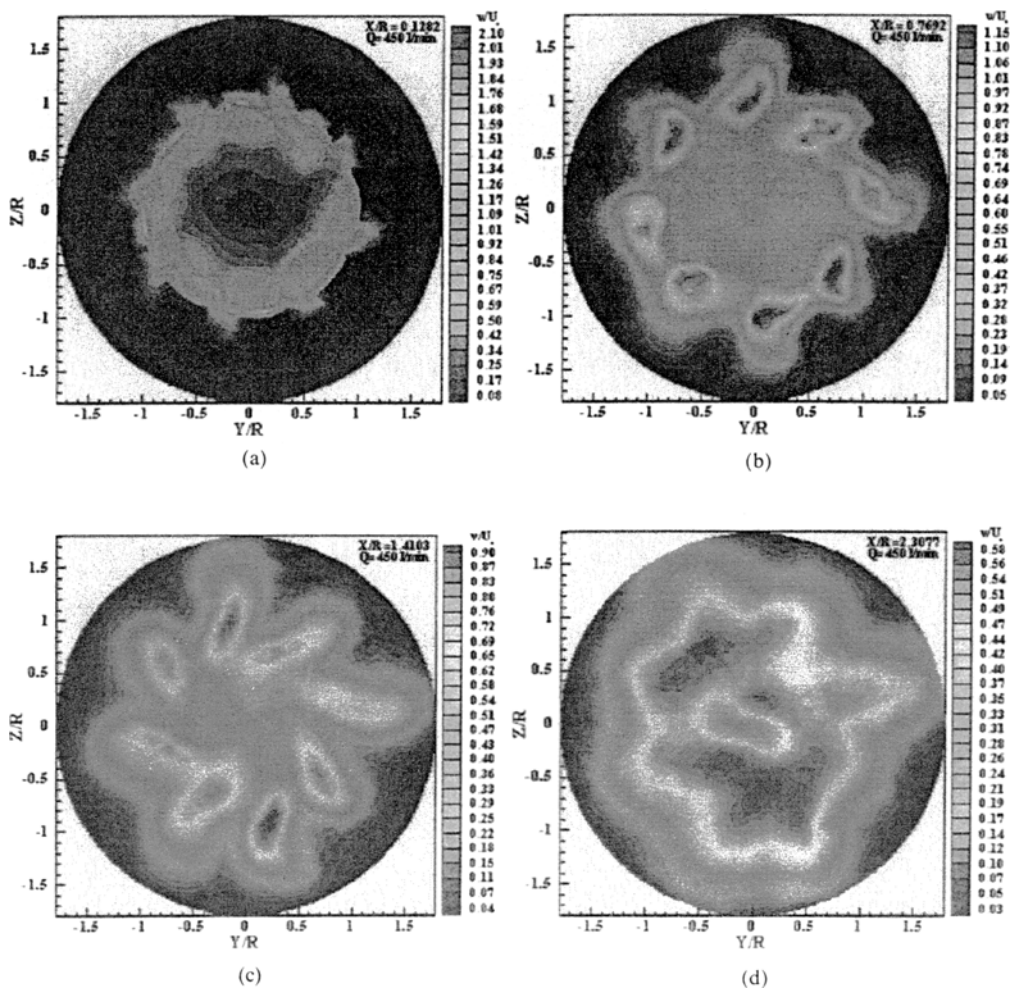

Fig. 6 Turbulent intensity v profiles in the Y-Z plane

Figure 6 shows the non-dimensional turbulent intensity distribution represented by dividing RMS v measured in the Y-Z plane at the location of X/R=0.1282, 0.7692, 1.4103 and 2.3077 respectively by upstream mean velocity U_0 of a swirl burner. The turbulent intensity v of Fig. 6(a) measured in the front of a burner appears to be fully developed with the large magnitude of above 200 % larger than that of u around r/R=0.97 corresponding to narrow slits. Particularly, the turbulent intensity v is largely distributed with above about 50 % between the range of $0.5<r/R<1$ and the outer region of a burner. Moreover, the turbulent intensity v in the central region of the burner appears to be reduced as the radial distance changes from the outer region to the origin, and also it shows a minimum value of about 10 % in the origin of a burner. As the axial distance increases, the turbulent intensity v around the narrow slits as shown in Fig. 6(b) forms a maximum value as well as the expanded range even though its magnitude is reduced. On the other hand, the maximum value of turbulent intensity v formed from the narrow slits as shown in Fig. 6(c) indicates an elongated shape toward the rotating flow direction as a result of the mixing between the flow going out of narrow slits and the flow rotation due to the swirl vanes in the internal region of a burner. Moreover, the turbulent intensity v shown in Fig. 6(d) indicates a magnitude of about 50 % covering entire region of a burner except a portion of the central region

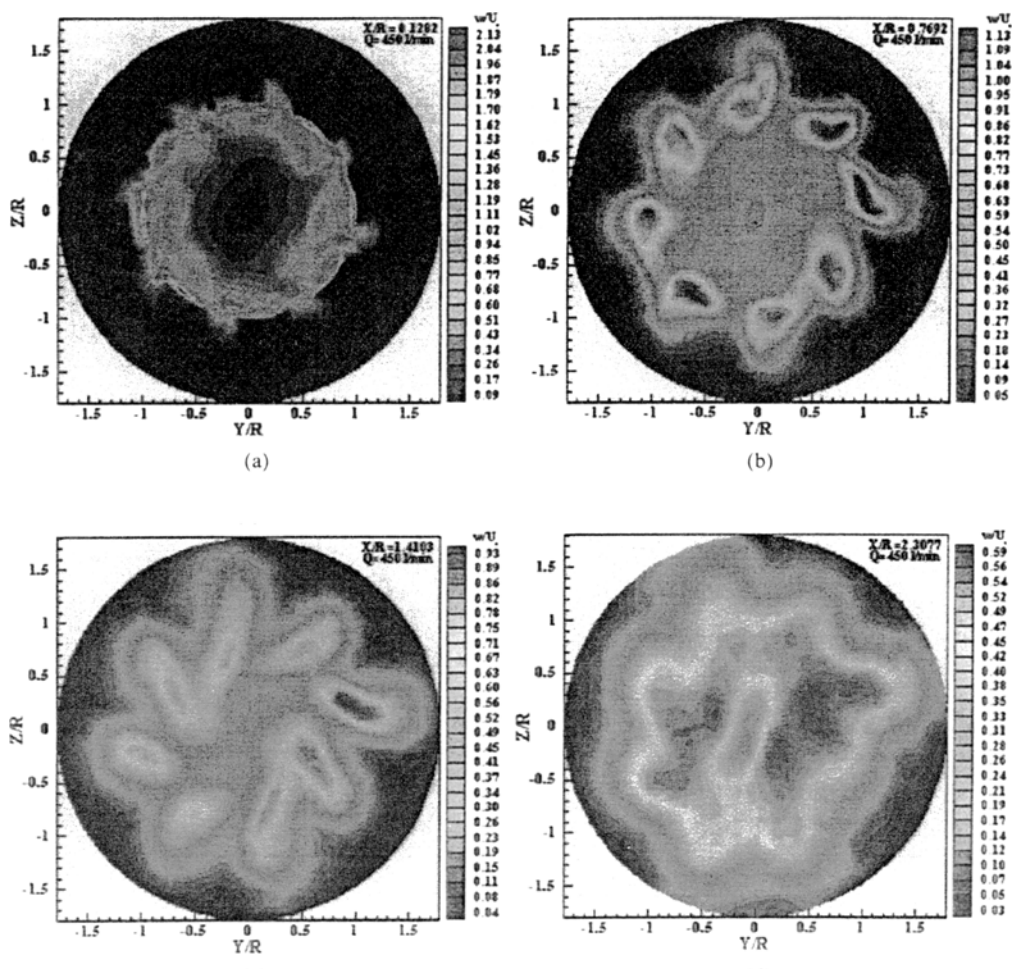

Fig. 7 Turbulent intensity w profiles in the Y-Z plane

because the flow comparatively fully develops.

Figure 7 shows the non-dimensional turbulent intensity distribution represented by dividing RMS w measured in the Y-Z plane at the location of X/R=0.1282, 0.7692, 1.4103 and 2.3077 respectively by upstream mean velocity U_0 of a swirl burner. The turbulent intensity w of Fig. 7 (a) measured in the front of a burner is also distributed with large value of above 210 % larger than that of u or v as the flow develops around r/R=0.97 corresponding to eight narrow slits. Moreover, the turbulent intensity w is largely distributed with a value of above about 60 % between the range of $0.5<r/R<1$ and the outer region of a burner. The turbulent intensity w in the central region of the burner is reduced as the radial distance changes from the outer region to the origin of a burner, and it shows a minimum value of about 10 % near the origin. On the other hand, as the axial distance increases, the turbulent intensity w as shown in Fig. 7(b) largely develops around the narrow slits, and the elongated shape of it toward the rotating flow direction can be seen in Fig. 7(c) because the reduced mean velocity U as well as the rotational flow due to the swirl vanes dominantly acts in this region, and then the mixing between the flow going out of narrow slits and the rotational flow going out of swirl vanes seems to actively progress in it. Moreover, the turbulent intensity w of Fig. 7(d) indicates a magnitude of about 50 % covering entire region of a burner except a portion of the

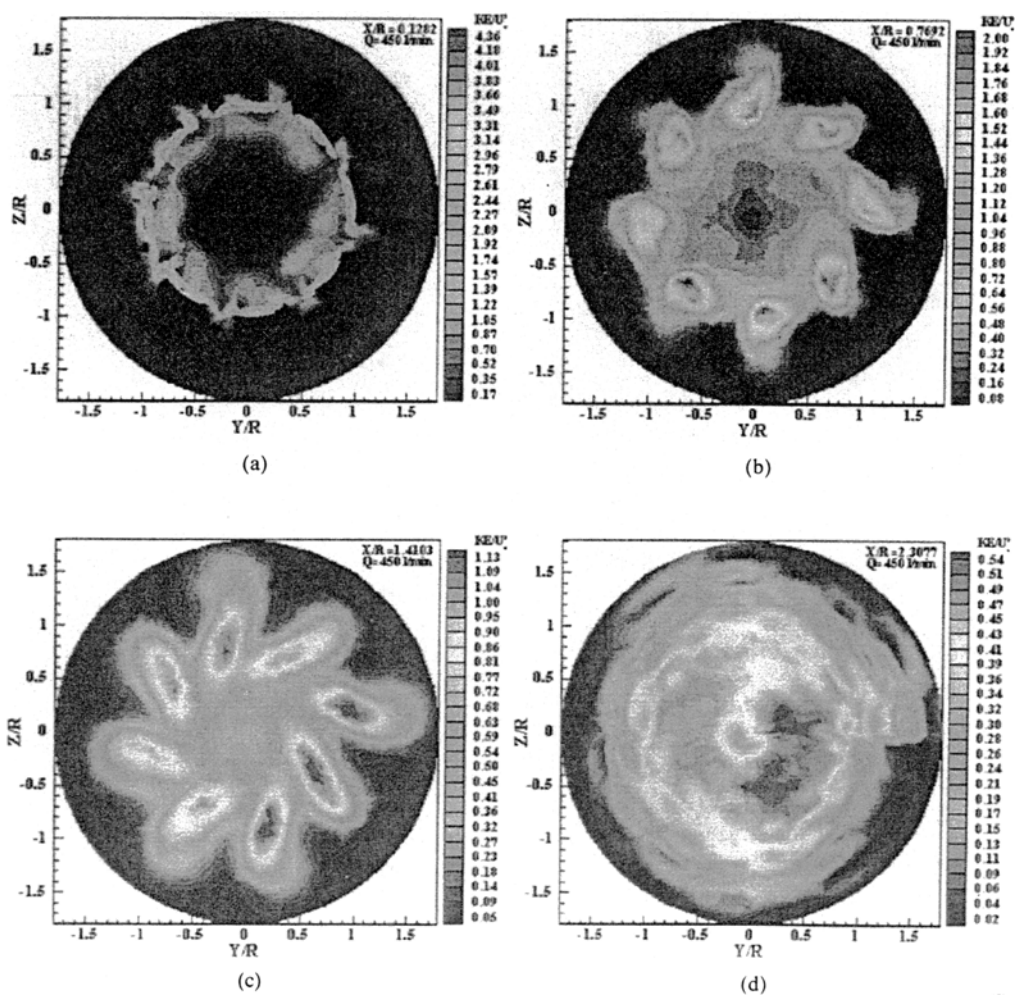

Fig. 8 Turbulent kinetic energy profiles in the Y-Z plane

central region because the flow comparatively fully develops.

4.3 Turbulent kinetic energy distribution

Figure 8 shows the distribution of non-dimensional turbulent kinetic energy described by dividing the turbulent kinetic energy obtained in the Y-Z plane at the location of X/R=0.1282, 0.7692, 1.4103 and 2.3077 respectively by upstream mean velocity U_0^2 of a swirl burner.

The turbulent kinetic energy obtained at the front of a burner as shown in Fig. 8(a) like a turbulent intensity indicates a distribution of the largest scale around r/R=0.97 corresponding to narrow slits, and the second large scale is distributed within the range of $0.5<r/R<1$ corresponding to the range between swirl vanes and narrow slits. However, as the axial distance increases, the turbulent kinetic energy can be seen in Fig. 8(b) that its range is widely expanded even though its scale is reduced around narrow slits. Therefore, the turbulent kinetic energy of Fig. 8(c) shows an elongated shape toward the rotating flow direction because both the flow going out of narrow slits and the rotational flow going out of swirl vanes develop and mix mutually in this region. On the other hand, the turbulent kinetic energy shown in Fig. 8(d) is widely distributed with a uniform value covering entire region of a burner.

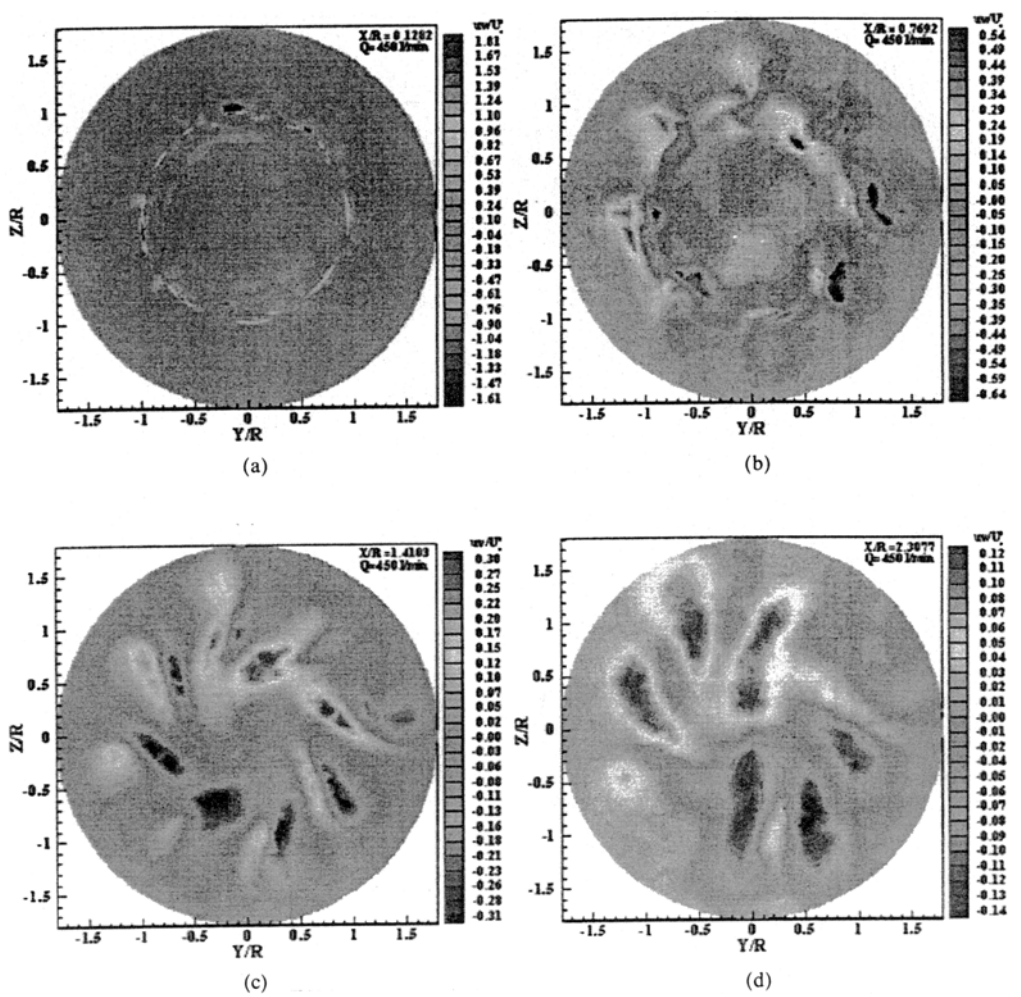

Fig. 9 Reynolds shear stress uv profiles in the Y-Z plane

4.4 Reynolds shear stress distribution

Figure 9 shows the distribution of non-dimensional turbulent shear stress described by dividing the Reynolds shear stress uv obtained in the Y-Z plane at the location of X/R=0.1282, 0.7692, 1.4103 and 2.3077 respectively by upstream mean velocity U_0^2 of a swirl burner. It can be seen that the Reynolds shear stress uv of Fig. 9(a) corresponding to the forefront of a burner is distributed with a large scale near eight narrow slits. Moreover, it can be considered that most of the magnitudes of Reynolds shear stress uv develop within the range of $0.5<r/R<1$. The negative and positive peak values of uv exist in the inner and outer parts of a burner respectively at Y/R=−0.97 corresponding to the left side of Fig. 9(a), and vice versa at Y/R=0.97 corresponding to the right side. This reason why the Reynolds shear stress uv appears differently in these regions is because the transverse slope of mean velocity with respect to the respective direction composing of uv acts differently. Here, the Reynolds shear stress uv simultaneously shows a distribution of the positive and negative values formed in the inner and outer region respectively with rotating clockwise around the narrow slits of a burner. Especially, the positive value of uv forms in the inner part of the top side of a burner with respect to Z-axis, and vice versa in the inner part of the lower side. As the axial distance increases, the positive and negative peak values of Reynolds shear stress uv stretch uniformly along the flow region cover-

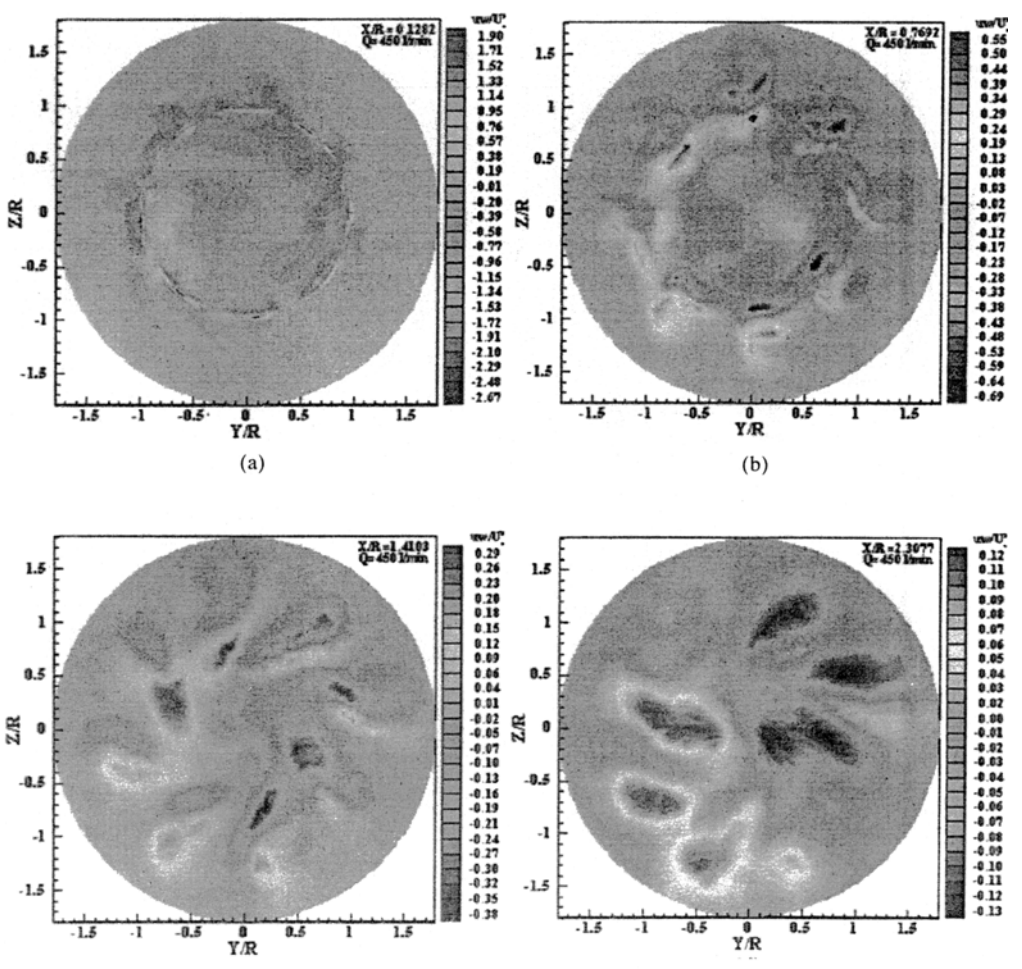

Fig. 10 Reynolds shear stress uw profiles in the Y-Z plane

ing the upper and lower sides of a burner as shown in Fig. 9(b) and Fig. 9(c) by means of the mixing between the jet flow of slits and the rotating flow of swirl vanes. Finally, the positive value of Reynolds shear stress uv shown in Fig. 9(d) exists in the top side of a burner, and vice versa in the lower side. Kihm et al. (1990) described that the Reynolds shear stress has both negative and positive values associated with the positive and negative gradients of the mean velocity profiles. For swirling flows, the turbulent shear stress distribution is strongly non-isotropic and is a function of the degree of swirl and position in the flow field. (Lilley et al., 1971)

Figure 10 shows the distribution of non-dimensional turbulent shear stress described by dividing the Reynolds shear stress uw obtained in the Y-Z plane at the location of X/R=0.1282, 0.7692, 1.4103 and 2.3077 respectively by upstream mean velocity U_0^2 of a swirl burner. The Reynolds shear stress uw obtained from X/R=0.1282 corresponding to the forefront of a burner such as Fig. 10(a) shows a distribution of a relatively large value as a result of the diffusion and development of flow toward the inner and outer parts respectively around the narrow slits. Besides the positive and negative peak values of uw exist in the inner and outer parts of a burner respectively at Y/R=−0.97 corresponding to the left side of Fig. 10(a), and vice versa at Y/R=0.97 corresponding to the right side. Here, the Reynolds shear stress uw is distributed with the positive and negative values formed in the inner and outer sides of a burner respectively with rotating clockwise around the narrow slits. Particularly, the negative value of uw is distributed in the inner part of the right side of a burner with respect to Y-axis, and vice versa in the inner part of the left side. The Reynolds shear stress uw shown in Fig. 10(b) and Fig. 10(c) indicates that both the positive and negative peak values are dominantly distributed in the left and right sides of a burner respectively, but their flow ranges are widely expanded, and also their scales are reduced because both the jet and the rotating flow develop and mix between the narrow slits and the swirl vanes. As the axial distance increases, it can be known that the positive and negative values of Reynolds shear stress uw as shown in Fig. 10(d) are widely distributed in the left and right sides respectively.

5. Conclusion

In consequence of the analysis of three-dimensional turbulent flow fields measured in the Y-Z plane of the gas swirl burner with a cone type baffle plate by using an X-probe of hot-wire anemometer system, the distributions of mean velocity show that the axial mean velocity is distributed with the largest scale around the narrow slits situated radially on the edge of a swirl burner. As the axial distance increases, the flow actively develops toward the inner and outer sides of a burner respectively because the axial mean velocity is remarkably reduced and the rotating flow due to the swirl vanes is relatively highlighted. The mean velocity V and W obtained from each axial distance have a magnitude of about 30 % smaller than U because of the rotating flow going out of the inclined swirl vanes situated on the surface of a cone type baffle plate. Moreover, the turbulent intensities show a large value changing from about 50 % to 210 % within the range of $0.5<r/R<1$ because the transverse slope of axial mean velocity is very largely distributed around these regions, and the swirl effect acts at the same time in these regions. Therefore, it can be expected that these regions produce a good condition of combustion because the intensive mixing between gas fuel and oxygen forms a high temperature around these regions when the burning is actually achieved. Moreover, the Reynolds shear stresses are also largely distributed in the inner and outer parts of a burner around narrow slits.

Acknowledgement

This paper is partially supported by the Fisheries Science Institute of Kunsan National University in 2000.

References

Aoki K., Nakayama Y. and Wakatsuki M., 1988, "Study on the Cylindrical Combustor Flow with Swirling Flow (1st Report, Characteristics of Flow Pattern for Swirling Number)," *Transactions of JSME (Part B)*, Vol. 51, No. 468, pp. 2759~2766 (In Japanese).

Aoki K., Shibata M. and Nakayama Y., 1989, "Study on the Cylindrical Combustor Flow with Swirling Flow (2nd Report, Characteristics of Turbulence for Swirling Number)," *Transactions of JSME (Part B)*, Vol. 52, No. 476, pp. 1617~1625 (In Japanese).

Beer J. M. and Chigier N. A., 1972, *Combustion Aerodynamics*, Applied Science Publishers, pp. 100~146.

Bruun H. H., 1996, *Hot-Wire Anemometry*, Oxford Science Publications, pp. 132~163.

Dantec, 2000, *Streamline User's Reference Manual*, Chapter 8.3 Algorithms.

Ikeda Y., Kawahara N. and Nakayima T., 1995, "Flux Measurements of O_2, CO_2 and NO in Oil Furnace," *Transactions of JSME (Part B)*, Vol. 61, No. 581, pp. 332~338 (In Japanese).

Kihm, K. D., Chigier, N., and Sun, F., 1990, "Laser Doppler Velocimetry Investigation of Swirler Flowfields," *J. Propulsion*, Vol. 6, No. 4, pp. 364 ~374.

Kim, I. K., 1997, "The Study on Flame Structure and Characteristics of Gun Type Burner for Different Type of Flame Holder," Master Thesis, Pusan National University, pp. 43~46 (In Korean).

Kim, I. K., Youn, W. H., Ha, M. Y. and Kim, Y. H., 1998, "The Study on Flow and Combustion Characteristics of Gun-Type Gas Burner," *Proceedings of the KSME Spring Annual Meeting B*, pp. 284~289 (In Korean).

Kim, J. K., 2001, "Investigation of the Three-Dimensional Turbulent Flow Fields of a Gas Swirl Burner with a Cone Type Baffle Plate (Ⅰ)," *KSME International Journal*, Vol. 15, No. 7, pp. 895~985.

Kim, J. K., Jeong, K. J., Kim, S. W. and Kim, I. K., 2000, "Investigation of the Three-dimensional Turbulent Flow Fields in Cone Type Gas Burner for Furnace," *Journal of KSPSE*, Vol. 4, No. 4, pp. 25~31 (In Korean).

Kim, J. K., 2001, "An Experimental Study on the Three Dimensional Turbulent Flow Characteristics of Swirl Burner for Gas Furnace," *Transactions of KSME (Part B)*, Vol. 25, No. 2, pp. 225~234 (In Korean).

Lilley, D. G. and Chigier, N. A., 1971, "Nonisotropic Turbulent Shear Stress Distribution in Swirling Flows from Mean Value Distributions," *International Journal of Heat and Mass Transfer*, Vol. 14, pp. 573~585.

Shigier, N., 1981, Energy, *Combustion and Environment*, McGraw-Hill, pp. 4~5.

Yoon, W. H., 1999, "The Numerical Study on the Flow and Combustion Characteristics of Gas Swirl Burner," Master Thesis, Pusan National University, pp. 7~39 (In Korean).